

Introduction

The most common type of mass loss of stars evolved away from the main-sequence is a “cool wind” as found for most red giants and supergiants of spectral type K and early M. However, despite several decades of research, the processes driving these winds are still poorly understood. These stars do not produce dust in sufficient quantities and have insufficient CS opacity to facilitate significant radiation pressure for mass loss — see, e.g., Schröder et al. (2003) for a model-based description of this kind of mass loss. Hence, the energy reservoir for driving these cool winds is most likely related to some type of turbulent energy density, within the chromosphere or underneath, possibly associated with the manifestation of (magneto-)acoustic waves (e.g., Musielak 2004, and references therein). While just a small fraction of this energy is required for initiating cool star winds, many details on the generation of non-radiative energy as well as the acceleration of winds in the upper chromospheric regions are still unsolved.

In the absence of any physical model of cool wind driving processes, the (semi-)empirical, so-called “Reimers law” or “Reimers formula” (Reimers 1975) has been the popular choice of a parameterized mass-loss description for cool winds not driven by dust since over 30 years. Albeit making a rather adequate representation of observed mass-loss rates over a broad range, i.e., between on the order of 10^{-9} and $10^{-6}M_{\odot} \text{ yr}^{-1}$, the original Reimers relation does not provide any realistic physical reasoning on how the mass loss is generated. This has fueled our motivation for an attempt to derive the Reimers relation based on a physical approach: it considers a detailed assessment of the energy reservoir of the turbulent chromosphere with particular emphasis on the action of Alfvén waves (Schröder & Cuntz 2005; Paper I). By doing so, we arrived at an improved relationship now of physical reasoning, which also overcame the most significant shortcoming of the original Reimers law, i.e., the variable fitting factor η_{R} .

A further motivation for an improved mass-loss description arises from the need for an accurate theoretical initial-mass / final-mass relation for stellar evolution models. This is, e.g., a pivotal requirement for a quantitative model of the galactic white dwarf population (e.g., Schröder et al. 2004), including their cooling times, an excellent galactic disk chronometer. Other applications include evolved stars in the stellar population, particularly their mass-loss histories (e.g., Schröder et al. 1999; Schröder & Sedlmayr 2001; Schröder & Pagel 2003).

In Schröder & Cuntz (2005), we re-derive the classic Reimers relation (see Sect. 2.1). However, within this derivation, two extra terms of moderate impact on the empirical mass-loss prediction arise: one dependent on the stellar effective temperature T_{eff} and the other on the stellar surface gravitational acceleration g_{*} , with the final result given as

$$\dot{M} = \eta \cdot \frac{L_{*}R_{*}}{M_{*}} \cdot \left(\frac{T_{\text{eff}}}{4000 \text{ K}} \right)^{3.5} \cdot \left(1 + \frac{g_{\odot}}{4300 \cdot g_{*}} \right) \quad (1)$$

with $\eta = 8 \cdot 10^{-14}M_{\odot} \text{ yr}^{-1}$, g_{\odot} as solar surface gravitational acceleration, and L_{*} , R_{*} , and M_{*} in solar units.

Herein, the two main points of consideration are the following. First, the surface-integrated mechanical energy flux at the bottom of the chromosphere is found to be proportional to $T_{\text{eff}}^{7.5}$. After a substitution of the stellar luminosity

L , which is proportional to T_{eff}^4 , a temperature-dependent term alike $T_{\text{eff}}^{3.5}$ is obtained. Though subtle, we found evidence for this extra term from the masses lost on the RGB by globular cluster stars of very different metallicity, as sensitively revealed by the colors of their present-day horizontal branch stars (see Schröder & Cuntz 2005).

Unfortunately, even the best-studied individual giants discussed below still come with uncertainties of their physical parameters too large, and a relative range of T_{eff} too small, to allow a direct assessment of the T_{eff} -exponent. Furthermore, different trial versions would require recalibrated η -values, which reduce the resulting difference in predicted mass loss.

The second extra term stems from the increase in characteristic chromospheric extent as function of decreasing stellar surface gravity, after substituting it by the stellar radius R_{*} , and it does make a noticeable difference with most stars studied here. Examples of large chromospheric extent include M-type supergiants (Hartmann & Avrett 1984; Airapetian et al. 2000). Considering the upper chromosphere as a starting point of the stellar wind, the implication is that a relatively low amount of potential energy is required to initiate the wind, if it starts further away from the photosphere. This term can make up to a factor of 2 to 3 for supergiants on the verge of a dust-driven wind, albeit not fully developed, as found in α Ori (M2 Iab), see Sect. 3.6.

Therefore, in the following, we make use of the best-studied galactic giants and supergiants, both in terms of stellar parameters and observed mass loss, to critically test our improved Reimers-type mass-loss relation. Our aim is to compare its predictions with the results of other mass-loss formulas given in the literature. The by far most accurate, empirical mass-loss determinations arise from a small number of giants and supergiants for which direct or indirect, as by means of an orbiting companion acting as a light probe, *spatial resolution of the circumstellar envelope* exists. This criterion yields a the sample of case studies presented below, with the exception of the old and very near RGB giant α Boo.

In Sect. 2, we present the other mass loss formulas from the literature used for this study, as well as information of the computation of the stellar evolution models and the statistical method to establish the uncertainty bars of the predicted mass loss rates. Section 3 lists our case studies and Sect. 4 presents our conclusions.

1. Approach

1.1. Empirical mass-loss formulas

For clarity, we concentrate on comparing our new relation only with the few, most commonly used mass-loss relations for cool winds. The popular, original “Reimers law”,

$$\dot{M} = \eta_{\text{R}} \cdot \frac{L_{*}R_{*}}{M_{*}} \quad (2)$$

has been conceived already over 30 years ago (Reimers 1975) [R75], in a time when the physical processes governing the initiation of mass loss in cool, low-gravity stars were virtually unknown. Consequently, Reimers never claimed any physical reason for this relation, as he rather based it on pure dimensional arguments. Kudritzki & Reimers (1978) later on calibrated η_{R} , the only free parameter, based on

observed mass-loss rates of three well-studied M-type supergiants, i.e., α Sco, α^1 Her, and δ^2 Lyr, deducing a value of $\eta_R = 5.5 \cdot 10^{-13}$. However, the wide-spread application of the ‘‘Reimers law’’, over the years, has seen the usage of a range of different values for η_R to fit mass-loss rates for a large variety of stars, which significantly diminished the significance of the proposed relation. In fact, the most commonly used value has been $\eta_R = 2 \cdot 10^{-13}$, which will be considered in the forthcoming comparisons.

Another early, purely empirical relation for was suggested by Lamers (1981) [L81] for O and B giants, which in terms of L_* , R_* , and M_* (in solar units) reads

$$\dot{M} = 10^{-4.83} \cdot \left(\frac{L_*}{10^6}\right)^{1.42} \cdot \left(\frac{R_*}{10^3}\right)^{0.61} \cdot \left(\frac{M_*}{10^0}\right)^{-0.99} . \quad (3)$$

While clearly not intended by the author for describing the mass loss of late-type giants and supergiants, it has nonetheless previously been used for this purpose. Therefore, we have included it for comparison.

De Jager et al. (1988) [dJNH88] presented an empirical formula based on Chebychev polynomials by which they obtained the best match of the mass-loss rates for a large sample of stars. In this case, the predicted mass-loss rates were given as functions of L_* and T_{eff} . In a subsequent paper, Nieuwenhuijzen & de Jager (1990) [NdJ90] presented a simpler parameterization to fit their updated sample, which again included stars of high luminosity. They found

$$\dot{M} = 9.63 \cdot 10^{-15} \cdot L_*^{1.42} \cdot R_*^{0.81} \cdot M_*^{0.16} . \quad (4)$$

However, from today’s perspective, it is noteworthy that this type of approach does not distinguish between the two main groups of cool giants and supergiants with very different mass-loss mechanisms, i.e., highly evolved cool supergiants with dust-driven winds, and less evolved giants and supergiants with cool winds *not* driven by radiation pressure on dust. This phenomenon results in an almost discontinuous change of the stellar mass-loss behavior as function of stellar luminosity, as e.g. also found in the empirical analysis by Judge & Stencel (1991). Furthermore, as a trade-off for their very large sample size, the individual stellar properties often lack precision. Additionally, these relationships were based on mass loss and luminosity determinations obtained prior to new developments such as improved angular diameter measurements, new stellar spectral analyses, and parallax determinations by Hipparcos.

1.2. Stellar evolution models

In order to complete the set of physical parameters, especially for deriving the stellar parameters L and T_{eff} of the giants and supergiants studied here, we have computed evolution tracks for finding the best-matching masses. For this purpose, we use a fast and well-tested evolution code (Eggleton 1971; Pols et al. 1997) in combination with a mass-loss description.

The evolution code and its semi-empirical choice of convection parameters has been tested very sensitively by means of supergiants in eclipsing spectroscopic binaries with well-known physical parameters (Schröder et al. 1997) allowing to deduce quantitatively reliable models for evolved stars. Furthermore, the evolution code readily accepts any mass-loss prescription as part of its boundary condition at each individual time-step (see Schröder et al.

1999). This is an ideal property for devising stellar evolutionary computations including the associated total mass loss (e.g., Schröder & Sedlmayr 2001; Schröder & Cuntz 2005). At the same time, a connection is obtained between the present-day mass and the initial mass for any highly evolved star with a cool wind, as e.g. undertaken for α^1 Her (see Sect. 3.5).

Most important for this work is, however, that the use of this well-calibrated evolution code helps us to test and further reduce uncertainties in the physical properties of the stars studied here. This is pivotal for assessing the various empirical mass-loss relationships, because rarely are there direct empirical constraints on (super-)giant’s masses. Also, when available, conflicting empirical constraints can leave us with alternative parameter sets.

1.3. Uncertainty bar analysis

An important aspect of any meaningful comparison between predicted mass-loss rates and observations or between themselves is the determination of uncertainty bars. In case of predicted mass-loss rates, these uncertainties evidently depend on the uncertainties of the input parameters. The various mass-loss relationships considered here constitute different function with some differences concerning their input parameters. Specifically, the mass-loss relations by Reimers (1975), Lamers (1981), and Nieuwenhuijzen & de Jager (1990) depend on L_* , R_* , and M_* (see Eqs. 2, 3, and 4), the relation by de Jager et al. (1988) depends on L_* and T_{eff} , and the new relationship by Schröder & Cuntz (2005) depends on L_* , R_* , T_{eff} , and M_* (see Eq. 1).

The uncertainty bars of these input quantities for the different stars, as well as the input quantities themselves, are carefully evaluated in Sect. 3, based on detailed observations and measurements. In that respect, it should be noted that out of L_* , R_* , and T_{eff} , only two variables are physically independent of each other. Therefore, the remaining parameter, if required, as well as its uncertainty bar, needs to be calculated from the two other parameters available. Furthermore, the surface gravity, as well as its uncertainty, used in the relation by Schröder & Cuntz (2005), is also not independent, but given by R_* and M_* .

In order to obtain the uncertainty of each predicted mass-loss rate for each star, we take the following approach: by utilizing a random number generator, we produce a random series of mass-loss rates X_{ij} for each case i (i.e., star or predicted mass-loss rate) by statistically varying the input data using a Gaussian distribution. The mean and the standard deviation for each input quantity are given by observations (see Sect. 3). The uncertainty bar for each case δX_i is then defined as

$$\delta X_i = \sqrt{\frac{\sum_{j=1}^n (X_{ij} - \bar{X}_i)^2}{n - 1}} \quad (5)$$

with \bar{X}_i as predicted mass loss rate and n as number of data for each case i . The random quantities X_{ij} were calculated by means of the standard routines `RAN1` and `GASDEV` (Press et al. 1986): `RAN1` delivers a uniform deviate of random numbers, which is used as input for `GASDEV`. `GASDEV` provides a normal deviate for a specified mean value and standard deviation. For each case, we produced a series of 50 runs.

Table 1. Recently published physical parameters of α Boo.

Source	d [pc]	$BC + A_v$	$\log L_*/L_\odot$	T_{eff} [K]	R_* [R_\odot]	M_* [M_\odot]	\dot{M}_{obs} [$M_\odot \text{ yr}^{-1}$]
JS91	$10.0 \pm 20\%$ **)	...	2.23 ± 0.2	$4250 \pm 5\%$ *)	$27 \pm 20\%$	$1.0 \pm 20\%$	$2.0 \cdot 10^{-10}$
GLG99	$11.3 \pm 2\%$ **)	...	2.22 ± 0.02	$4290 \pm 1\%$	$23 \pm 2\%$ *)	$1.0 \pm 20\%$...
DVW03	$11.3 \pm 2\%$ ***)	...	2.29 ± 0.07	$4320 \pm 3\%$ *)	$25 \pm 6\%$	$1.2 \pm 50\%$...
adopted:	$11.3 \pm 2\%$	0.55 ± 0.05	2.23 ± 0.02	$4290 \pm 1\%$	$23 \pm 6\%$ *)	$1.10 \pm 6\%$	$2.5 \cdot 10^{-10}$

Notes: *) derived value within the set L_* , T_{eff} , R_* (see text), **) using spectrophotometry, ***) using IR photometry. A colon (:), if given, indicates a value with an unknown error bar, which in some cases may be relatively large.

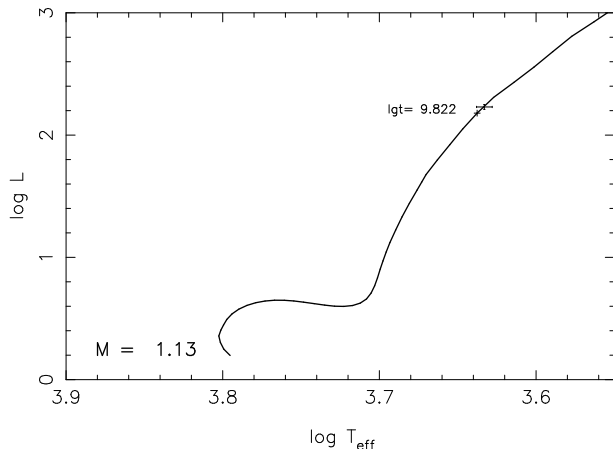


Fig. 1. Luminosity versus effective temperature for stellar evolution computations of Arcturus. Note that the observationally deduced value of T_{eff} is very well matched for an evolution track of $1.13M_\odot$ with subsolar metallicity of $Z = 0.01$, implying an age of $6.6 \cdot 10^9$ yr.

2. Individual case studies

2.1. α Boo (K1.5 III)

The star α Boo has long been known as a mildly metal-poor giant with $[\text{Fe}/\text{H}] = -0.50$ (Decin et al. 2003) [DVW03]. Spectrophotometry yields $T_{\text{eff}} = 4290$ K (Griffin & Lynas-Gray 1999) [GLG99], which is accurate within approximately 50 K. As previously suggested by Charbonnel et al. (1998), Arcturus is probably an old, low-mass RGB giant: the metal-poor RGB coincides with the AGB of solar abundance in T_{eff} , whereas a low-mass star spends a significant time on the RGB, making this solution by far the most likely one. Furthermore, α Boo’s proximity allows a precise distance measurement (by Hipparcos) of $d = 11.3$ pc and permits very accurate physical parameter determinations. All this makes α Boo a very interesting case; however, it differs from the other objects considered that its observed mass-loss rate has not been derived from a spatial resolution study. Hence, it remains more uncertain.

With $V = -0.04$, a distance modulus of 0.26, and $BC = 0.55$, Arcturus has a luminosity of $170 L_\odot$, or $M_{\text{bol}} = -0.85$, which yields a flux-related radius of $23 R_\odot$, consistent with that given by Griffin & Lynas-Gray (1999), and corresponding to an angular diameter of $\theta = 18.9$ mas (see Table 1). This is in very good agreement with the

LBI (Long Baseline Interferometry) uniform disk diameter (hereafter referred to as UDD), as in visual light, UDDs of 19.0 ± 0.2 mas and 21.0 ± 0.3 mas have been measured (Richichi & Percheron 2002). Note that we compare UDDs and flux radii in a consistent manner for all stars for reasons of simplicity. In fact, giant and supergiant radii are ill-defined quantities which are often critically dependent on how they were derived. This becomes particularly obvious for α Ori (see Sect. 3.6).

As a RGB giant, Arcturus’ luminosity and its effective temperature is fitted best by an evolution track for $1.13 M_\odot$, using a reduced metallicity of $Z = 0.01$ (see Fig. 1). RGB stars of masses within $\pm 0.05 M_\odot$ of that value would still be within an uncertainty of T_{eff} of 1%. Considering the possible miss-match between the grid metallicity used and the observed $[\text{Fe}/\text{H}]$ value for Arcturus — slightly lower and close to $Z = 0.007$ — we arrive at a slightly lower mass of $1.10 M_\odot$, with a total error of $\pm 0.06 M_\odot$. Based on these values, we obtain a surface gravity of $\log g = 1.76 \pm 0.05$ (cgs); see Table 7 for a summary of the adopted parameters.

For the above set of parameters, the new relation by Schröder & Cuntz (2005) with a calibrated value of $\eta = 0.8 \cdot 10^{-13}$ suggests a mass-loss rate of $4.0 \cdot 10^{-10} M_\odot \text{ yr}^{-1}$. This is well within the uncertainty range of the observed mass-loss rate, while the old “Reimers law” (with a re-calibrated value of $\eta_{\text{R}} = 2 \cdot 10^{-13}$) as well as all other relations but one (see Table 8) result in much larger discrepancies.

As for the observed mass-loss rate, radio continuum emission measures at 6 cm and 2 cm wavelength yielded ionized mass-loss rates between $6.9 \cdot 10^{-11}$ and $8.4 \cdot 10^{-11} M_\odot \text{ yr}^{-1}$ (Drake & Linsky 1983, 1986). As far as the total mass-loss rate is concerned, we would need to know the average ionization ratio of the CS envelope. However, no sophisticated model exists for the CS matter, where the radio emission originates. But we may speculate that, due to radiative cooling and NLTE processes, the ionization fraction decreases considerably from close to 100% in the mid chromosphere to low values further out in the wind (Ayres & Linsky 1975; Cuntz 1990). Indeed, Ayres et al. (2003) presented observational evidence that the circumstellar matter of Arcturus is acting as a “cool absorber” to the radiative emission of the hot chromospheric gas buried beneath. This would imply a smaller ionization degree further outward, indicating a larger total mass-loss rate than the ionized mass loss obtained from the above radio observations.

In their study of a number of cool giants with mass loss, Judge & Stencel (1991) [JS91] adopted a value of $2.0 \cdot 10^{-10} M_\odot \text{ yr}^{-1}$ for the total mass loss of Arcturus, as originally derived by Drake (1985) from Mg II emission line profile modelling and in line with the aforesaid. Correcting their

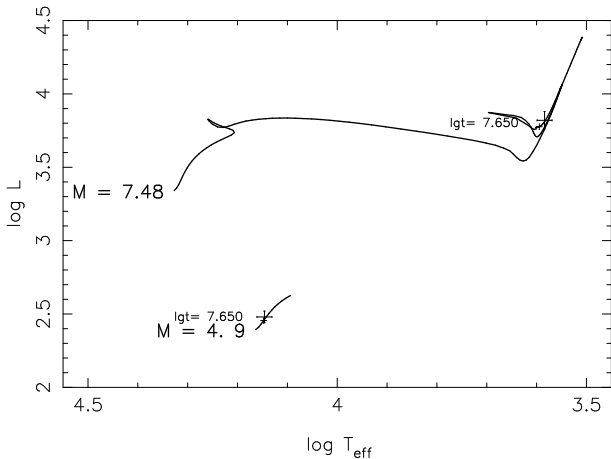


Fig. 2. The observed HRD positions of both components of the ζ Aur-type system 32 Cygni are matched very well by evolution tracks of $4.13 M_{\odot}$ and $7.58 M_{\odot}$ (initial) mass, at an age of $4.4 \cdot 10^7$ yr, using an enhanced metallicity of $Z = 0.03$.

distance value of 10.0 pc to the actual distance of 11.3 pc translates into a mass-loss rate of $2.5 \cdot 10^{-10} M_{\odot} \text{ yr}^{-1}$ — noting that these measures are based on areal (angular) emission and, hence, the derived mass-loss rates scale with the distance squared.

While Mg II is probably the dominant ionization stage of Mg in most of the CS envelope, it is well-known that there are large ambiguities in the line modelling process. For example, different choices of turbulent velocity can all well result in good matches of the observed line profile, however, nonetheless corresponding to different mass-loss rates. Hence, we consider the above discussed rate to be uncertain by at least a factor of 2.

2.2. 32 Cyg (K5 Ib)

The wind of 32 Cyg, a K5 supergiant belonging to a spectroscopic binary system, has been well studied by means of the hot main sequence companion (Baade 1998, 1990a) by using IUE and HST spectra. The flux of the secondary dominates the UV spectrum of the binary and, hence, it acts as an orbiting light source, allowing to probe the circumstellar matter in the line of sight. Compared to the very similar ζ Aur and 31 Cyg supergiants, the 32 Cyg system has the least hot B star companion. Therefore, ionization effects by its radiation are less severe and less likely to affect any mass-loss rates derived from observation.

A mass-loss rate of 32 Cyg of $1.5 \cdot 10^{-8} M_{\odot} \text{ yr}^{-1}$ has been obtained by Baade (1990a, b) from high-resolution IUE spectra by modelling the resonance line scattering of singly ionized metals. Baade et al. (2001) revised this value to $1.3 \cdot 10^{-8} M_{\odot} \text{ yr}^{-1}$ while considering high-resolution HST spectra. The residual uncertainty of this rate is mainly caused by considerable intrinsic variability and chromospheric density fluctuations (see Wright 1970, Schröder 1983, Baade et al. 2001). We estimate it to be within a factor of about 1.6.

The eclipse geometry of 32 Cyg presents the peculiar complication that the secondary’s projected path grazes the limb of the giant. Hence, the eclipse geometry does not yield the radii, but it gives the inclination of the system for given mass ratio and giant radius. In order to determine the physical parameters, we can also consider (1) the mass function of the giant’s radial velocity curve, 0.301 (Wright 1970), which constrains the masses and their mass ratio q , (2) the semi-major axis $a_1 \sin i$ of the primary orbit of $2.55 \cdot 10^8$ km (Wright 1970), and (3) the effective temperature of the secondary of 14,000 K, well-determined by UV spectroscopy, and its angular diameter of 0.077 mas (Erhorn 1990, taking extinction into account), as well as (4) the effective temperature of 3840 K of the primary. The latter value was found by Levesque et al. (2005) [LMO05] from a comparison of the G-Band with MARCS stellar atmospheres. Table 2 compares the physical parameters and mass-loss rates adopted for the giant from earlier publications, i.e., Che et al. (1983) [CHR83], Baade (1990a, 1990b) [B90], and Baade et al. (2001) [B01], with this paper.

Hipparcos measured a parallax of $\pi = 2.94 \pm 0.6$ mas. It puts 32 Cyg at a distance of 340 (+90/-60) pc, smaller than the 383 pc suggested by CHR83. Since large relative parallax errors are asymmetric in distance, measured distances appear, on average, a little smaller (“Malmquist bias”), see Malmquist (1936). Hence, we find $d = 360$ pc a more likely value, from which for the secondary a radius of $3.0 R_{\odot}$ and a luminosity of $302 L_{\odot}$ is derived. For the primary ($V = 4.0$), we adopt $L_* = 6600 L_{\odot}$, which results from a radius of $184 R_{\odot}$ and from $T_{\text{eff}} = 3840$ K, and which is consistent with $BC + A_v = 1.05$. The corresponding $\theta = 4.75$ mas is then in excellent agreement with the UDD, measured by LBI, of 4.8 ± 0.1 mas listed by Richichi & Percheron (2002).

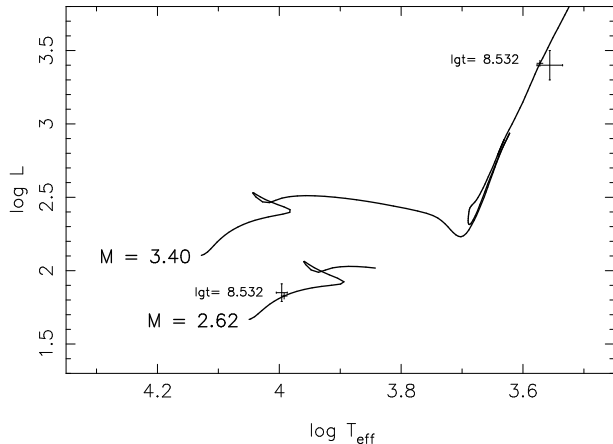
Next, we review the system parameters of 32 Cyg by means of evolution models, which are constructed to match the HRD positions of both stars for their well enhanced metallicity (Taylor 1999), and taking into account the equal age of both components. At the same time, eclipse geometry and mass function must be satisfied as well. A detailed description of this method has been presented by Schröder et al. (1997). We find that the secondary is fitted best by an evolution track with a mass of $4.13 M_{\odot}$, while the primary requires an initial mass of around $7.58 M_{\odot}$ (as shown in Fig. 2). This mass is reduced by mass loss, as given by the relation of Schröder & Cuntz (2005), to $7.46 M_{\odot}$ by the time the star has reached about the end of its core helium burning, i.e., after $4.4 \cdot 10^7$ yr of age. These mass values reproduce the mass function and the eclipse geometry very well with $q = 1.80$ and $i = 80^{\circ}$. This good multiple match not only yields the masses of the 32 Cyg components with unprecedented accuracy, it also reduces considerably the uncertainties of luminosity, radius and T_{eff} (see Table 2 for estimated errors).

With a mass of $7.45 M_{\odot}$ and a radius of $184 R_{\odot}$, the surface gravity of the 32 Cyg giant is $\log g = 0.78$ (cgs). The predicted mass-loss rates, as given by the relation of Schröder & Cuntz (2005) and by various other formulas (see Sect. 2.1), are compared in Table 8. The law by Schröder & Cuntz (2005) suggests a mass-loss rate of $2.3 \cdot 10^{-8} M_{\odot} \text{ yr}^{-1}$, which is consistent with the observed value. The original “Reimers law” (with $\eta_R = 2 \cdot 10^{-13}$), however, suggests $3.2 \cdot 10^{-8} M_{\odot} \text{ yr}^{-1}$, which is more than a factor of 2 above the observed value. The predictions by the other mass-loss relations disagree by much larger factors

Table 2. Recently published physical parameters of 32 Cyg.

Source	d [pc]	$BC + A_v$	$\log L_*/L_\odot$	T_{eff} [K]	R_* [R_\odot]	M_* [M_\odot]	\dot{M}_{obs} [$M_\odot \text{ yr}^{-1}$]
CHR83	$383 \pm 10\%$	1.0	3.82 ± 0.2 *)	$3800 \pm 5\%$	$188 \pm 10\%$	$8.0 \pm 15\%$	$2.8 \cdot 10^{-8}$
B90, B01	...	1.0	3.82 ± 0.02 *)	$3800 \pm 5\%$	$188 \pm 10\%$	$8.0 \pm 15\%$	$1.3 \cdot 10^{-8}$
adopted:	$360 \pm 5\%$	1.05 ± 0.07	3.82 ± 0.08 *)	$3840 \pm 3\%$	$184 \pm 6\%$	$7.45 \pm 4\%$	$1.3 \cdot 10^{-8}$

Notes: See Table 1.

**Fig. 3.** Observed HRD positions of the components of δ Sge and evolution tracks of $2.62 M_\odot$ and $3.40 M_\odot$ (initial) mass, using a metallicity of $Z = 0.02$.

(see Table 8), and are well outside the combined observational and theoretical uncertainty bars.

2.3. δ Sge (M2 II)

The star δ Sge A is a moderate mass AGB giant, and it is a member of a non-eclipsing spectroscopic binary system. Spectro-photometry has been carried out for the A0-type companion. The radial velocity measurements for both components imply an observed mass ratio of about 1:1.27 (Griffin, private communication). In addition, separation measurements by speckle interferometry exist for various phases indicating an inclination of $i = 40^\circ$ and a distance of about 180 pc. A study for δ Sge A based on these observations and on matching evolution tracks (Schröder et al. 1997) [SPE97] suggested a luminosity of $\log L_*/L_\odot = 3.57$ (with $V = 3.95$ and $BC = 1.75$), an effective temperature of $T_{\text{eff}} = 3600$ K, a radius of $R_* = 157 R_\odot$, and a mass of $M_* = 3.4 M_\odot$.

However, the Hipparcos parallax of δ Sge suggests a distance of 137 (+18/-14) pc. Hence, we adopt a distance of 150 pc ($m - M = 5.73$), which is fully consistent with a B star radius of $2.85 M_\odot$, considering a spectro-photometrically determined temperature of $T_{\text{eff}} = 9900$ K and angular diameter of 0.178 mas of the companion, Erhorn 1990). Therefore, we adopt the same T_{eff} of 3600 K for the δ Sge giant as used in that study. Furthermore, with $BC = 1.75$ and an estimated extinction (IS and CS combined) of $A_v = 0.25$, we derive a primary luminosity of

$\log L_*/L_\odot = 3.40$ (or $M_{\text{bol}} = -3.68$) and a (flux-) radius of $R_* = 129 R_\odot$. This yields an angular diameter of $\theta = 7.8$ mas, in excellent agreement with the LBI measurement of best accuracy for the UDD (7.8 ± 0.3 mas) listed by Richichi & Percheron (2002).

We estimate the remaining uncertainties to be 10% for the geometry (R_* , d) and mass, 8% for T_{eff} , and 20% for L_* . Within these uncertainties, the above physical parameters are well matched by evolution tracks (for $Z = 0.02$ and accounting for mass loss) for today's component masses of about 2.62 and $3.35 M_\odot$ (see Fig. 3). The relatively low luminosity of the M2 primary alone would rather suggest a lower mass of $\approx 3 M_\odot$, but this value is incompatible with the finding that the secondary component is not sufficiently advanced in its main-sequence evolution. Hence, we thus arrive at a surface gravity of $\log g = 0.74 \pm 0.10$ (cgs).

The mass loss of δ Sge has been observed by means of wind lines in the UV spectrum of the companion probing the wind at different phases without any significant ionization by its radiation. Reimers & Schröder (1983) [RS83] found rates of $1.8 \cdot 10^{-8} M_\odot \text{ yr}^{-1}$ for a phase close to conjunction (July 31, 1980), and of $2.5 \cdot 10^{-8} M_\odot \text{ yr}^{-1}$ (March 30, 1982) using IUE high resolution spectra. Back then, Reimers & Schröder assumed a much more inclined geometry (with $i = 70^\circ$), implying a line-of-sight which passes too close by the primary in the July '80 phase. With an approximate correction for an inclination of $i = 40^\circ$, both quoted phases imply a mass-loss rate of about $2.5 \cdot 10^{-8} M_\odot \text{ yr}^{-1}$.

But, in addition, Reimers & Schröder assumed a larger mass ratio of $\mu \approx 3$. Since the relative orbit size a is scaled with $(1 + \mu)$, and since the wind-line interpretation mainly depends on the absorbing column density, the derived densities (n) scale, roughly, as $(1 + \mu)^{-1}$ and the mass-loss rates ($\propto n \cdot v_w \cdot a^2$) as $(1 + \mu)$, with v_w as wind speed. Hence, for a much smaller mass-ratio of $\mu = 1.27$, we finally arrive at an updated mass loss of $1.4 \cdot 10^{-8} M_\odot \text{ yr}^{-1}$ (see Table 3). We estimate this rate to be uncertain by a factor of 2, mainly due to intrinsic variability of the outflow (e.g., Reimers & Schröder 1983) and remaining uncertainties in population ratios due to ionization and excitation processes.

For the above parameters, the mass-loss relation by Schröder & Cuntz (2005) yields a rate of $1.15 \cdot 10^{-8} M_\odot \text{ yr}^{-1}$, lower than the observational value but well within the range of uncertainty, while the old ‘‘Reimers law’’ (with $\eta_R = 2 \cdot 10^{-13}$) suggests a higher rate of $1.9 \cdot 10^{-8} M_\odot \text{ yr}^{-1}$. See Table 8 for the other rates, which are all significantly larger.

2.4. α Sco (M1.5 Iab)

The star α Sco A, Antares, is very similar to Betelgeuse (see Sect. 3.6) in mass, luminosity and spectral type —

Table 3. Recently published physical parameters of δ Sge.

Source	d [pc]	$BC + A_v$	$\log L_*/L_\odot$	T_{eff} [K]	R_* [R_\odot]	M_* [M_\odot]	\dot{M}_{obs} [$M_\odot \text{ yr}^{-1}$]
RS83	$170 \pm 25\%$	1.62	3.43 ± 0.2 *)	$3600 \pm 5\%$	$140 \pm 25\%$	8:	$2.0 \cdot 10^{-8}$
SPE97	$182 \pm 25\%$	1.81	3.57 ± 0.2 *)	$3600 \pm 5\%$	$157 \pm 25\%$	$3.4 \pm 10\%$...
adopted:	$150 \pm 10\%$	2.0 ± 0.2	3.40 ± 0.10 *)	$3600 \pm 8\%$	$129 \pm 10\%$	$3.35 \pm 10\%$	$1.4 \cdot 10^{-8}$

Notes: See Table 1.

Table 4. Recently published physical parameters of α Sco.

Source	d [pc]	$BC + A_v$	$\log L_*/L_\odot$	T_{eff} [K]	R_* [R_\odot]	M_* [M_\odot]	\dot{M}_{obs} [$M_\odot \text{ yr}^{-1}$]
KR78	$180 \pm 15\%$	2.0	4.68	$3550 \pm 10\%$	$575 \pm 20\%$ *)	18:	$0.7 \cdot 10^{-6}$
HN83	$180 \pm 15\%$	$2.0 \cdot 10^{-6}$
HHR87	$180 \pm 15\%$	2.0	4.68	$3550 \pm 10\%$	$575 \pm 20\%$ *)	18:	$1.0 \cdot 10^{-6}$
adopted:	$180 \pm 15\%$	2.0 ± 0.2	4.76 ± 0.12	$3400 \pm 6\%$	$703 \pm 15\%$ *)	$12 \pm 20\%$	$1.5 \cdot 10^{-6}$

Notes: See Table 1.

only slightly hotter and, presumably, a bit more massive. Its distance is well known (180 pc, $\pi = 5.4 \pm 1.7$ mas) and its circumstellar envelope is probed by a hot (18,500 K) but distant (2.9" angular separation) companion on the near side of its orbit. Kudritzki & Reimers (1978) [KR78] used optical wind absorption lines in the spectrum of the companion and simple ionization considerations to derive a mass-loss rate of $7 \cdot 10^{-7} M_\odot \text{ yr}^{-1}$ for α Sco A. Due to the wide orbit of the binary system, radiative ionization by the B2.5 V companion concerns only a small part of the cool wind. Hence, this star can accurately be modelled, including the height-dependent ionization degree in the line of sight (van der Hucht et al. 1980).

Hagen et al. (1987) [HHR87] used IUE spectra and re-determined the mass-loss rate from carefully selected, not blended circumstellar absorption lines in the spectrum of α Sco B. They found a value of about $1.0 \cdot 10^{-6} M_\odot \text{ yr}^{-1}$, with a remaining uncertainty of a factor of 2. From spacially resolved radio observations with VLA, a very different approach, Hjellming & Newell (1983) [HN83] deduced a mass loss rate of about $2.0 \cdot 10^{-6} M_\odot \text{ yr}^{-1}$ with a similar uncertainty. Hence, we adopt an observed mass-loss rate for α Sco A of about $1.5 \cdot 10^{-6} M_\odot \text{ yr}^{-1}$ (see Table 4).

The physical parameters of the supergiant α Sco A are fairly well constrained. Here we adopt $V \approx 1.02$ (variable), $m - M = 6.28$, a combined BC and A_v of 2.0 (similar to 2.1 for α Ori, see below), resulting in $M_{\text{bol}} = -7.2$ and $\log L_*/L_\odot = 4.76(\pm 0.12)$. Spectral type and $V - K$ index are only slightly earlier (smaller) than those of α Ori, indicating that its effective temperature should be slightly higher. Compared to the purely empirical, UDD-based α Ori Model A (see below), for α Sco A we should expect a $T_{\text{eff}} \simeq 3400$ K (± 200 K), giving a flux radius of $R_* = 703 R_\odot$, with an estimated error of 15%, and $\theta = 36.4$ mas. This value is in good agreement with the LBI-measured UDDs of α Sco A, which range from 29 to 45 mas (Richichi & Percheron 2002) and with the $V - K$ -related value of 37.7 mas by the same authors.

For a mass of approximately $12 M_\odot$, as indicated by our best-matching evolution model, the surface gravity of α Sco A is $\log g = -0.18 \pm 0.11$ (cgs). With these values,

the mass-loss relation by Schröder & Cuntz (2005) yields a rate of $1.5 \cdot 10^{-6} M_\odot \text{ yr}^{-1}$, in perfect agreement with the observed value, while the old “Reimers law” (with $\eta_R = 2 \cdot 10^{-13}$) predicts $6.6 \cdot 10^{-7} M_\odot \text{ yr}^{-1}$, a rate that is much too small (see Table 8 for the results from other relations).

2.5. α^1 Her (M5 Ib)

The wind of α^1 Her, a M-type supergiant, is just below the critical luminosity for becoming dust-driven (see Schröder et al. 1999). Its physical structure is probed by a spatially well resolved companion star, α^2 Her, separated by 4.7" from its primary. Reimers (1977) [R77] adopted a distance of 59 pc and a mass-loss rate of $\dot{M} = 1.1 \cdot 10^{-7} M_\odot \text{ yr}^{-1}$ from the wind absorption lines. These are seen in the composite spectrum of α^2 Her, itself a spectroscopic binary (i.e., α^2 Her A & B).

A detailed study was provided by Thiering & Reimers (1993) [TR93]. They used IUE spectra for deriving the component’s brightnesses and effective temperatures. Their mass-loss rate of the M supergiant is based on the line-of-sight line absorption by using mass column densities and the wind velocity structure, also considering ionization effects. For a distance of $d = 70$ pc, they found $\dot{M} = 1.5 \cdot 10^{-7} M_\odot \text{ yr}^{-1}$ with a 20% uncertainty (see Table 5). Mauron & Caux (1992) used observations of spatially resolved K I and Na I line scattering to derive an update value of $\dot{M} = 1.0 \cdot 10^{-7} M_\odot \text{ yr}^{-1}$, assuming a distance of 60 pc. Since all historic distance values of α^1 Her seem to be gross underestimates, according to modern measurements (see below), a significant adjustment of these observed mass-loss rates is required.

The Hipparcos parallax ($\pi = 8.5 \pm 2.8$ mas) now results in a distance of 120 pc (± 30 pc) for the α Her system. In fact, this value is perfectly consistent with a radius of $3.2 \pm 0.1 R_\odot$ for the A9 V star α^2 Her B with $T_{\text{eff}} = 7350$ K and $\log L_*/L_\odot = 1.49$, as previously derived by Thiering & Reimers (1993) from $V = 6.6$, $M - m = -5.4$, $A_v = 0.1$, and

Table 5. Recently published physical parameters of α^1 Her.

Source	d [pc]	$BC + A_v$	$\log L_*/L_\odot$	T_{eff} [K]	R_* [R_\odot]	M_* [M_\odot]	\dot{M}_{obs} [$M_\odot \text{ yr}^{-1}$]
R77	59:	3.2	...	$2880 \pm 10\%$ *)	$140 \pm 25\%$	8:	$1.0 \cdot 10^{-7}$
TR93	70:	3.2	...	$2880 \pm 10\%$ *)	$157 \pm 25\%$	$3.4 \pm 10\%$	$1.5 \cdot 10^{-7}$
LMO05	$(120 \pm 15\%)$	3.9:	4.33	3450:	410: *)
adopted:	$120 \pm 15\%$	2.9 ± 0.4	3.92 ± 0.15	$2800 \pm 10\%$ *)	$387 \pm 20\%$	$2.15 \pm 10\%$	$3.0 \cdot 10^{-7}$

Notes: See Table 1. L_* and R_* of [LMO05] are based on $d = 120$ pc, according to the Hipparcos parallax.

Table 6. Recently published physical parameters of α Ori.

Source	d [pc]	$BC + A_v$	$\log L_*/L_\odot$	T_{eff} [K]	R_* [R_\odot]	M_* [M_\odot]	\dot{M}_{obs} [$M_\odot \text{ yr}^{-1}$]
JS91	200:	**)	5.0:	3900: *)	860:	10:	$4 \cdot 10^{-6}$:
HBL01	$131 \pm 20\%$	**)	4.73 ± 0.15	$3140: *$	$789 \pm 20\%$...	$3.1 \cdot 10^{-6} \pm 40\%$
LMO05	$(131 \pm 20\%)$	2.2 ± 0.3	4.81 ± 0.15	3650:	637: *)
Model A	$131 \pm 20\%$	2.1 ± 0.3	4.73 ± 0.15	$3340 \pm 6\%$ *)	$695 \pm 20\%$	$10 \pm 20\%$	$3.1 \cdot 10^{-6} \pm 40\%$
Model B	$131 \pm 20\%$	2.2 ± 0.3	4.81 ± 0.15	$3650 \pm 10\%$	$637 \pm 20\%$ *)	$10 \pm 20\%$	$3.1 \cdot 10^{-6} \pm 40\%$

Notes: See Table 1. L_* and R_* of [LMO05] are based on $d = 131$ pc, according to the Hipparcos parallax.

Table 7. Adopted physical parameters for the various stars.

Object	d [pc]	$\log L_*/L_\odot$	T_{eff} [K]	R_* [R_\odot]	M [M_\odot]	$\log g_*$
α Boo	$11.3 \pm 2\%$	2.23 ± 0.02	$4290 \pm 1\%$	$23 \pm 6\%$	$1.10 \pm 6\%$	1.76 ± 0.05
32 Cyg	$360 \pm 5\%$	3.82 ± 0.08	$3840 \pm 3\%$	$184 \pm 6\%$	$7.45 \pm 4\%$	0.78 ± 0.06
δ Sge	$150 \pm 10\%$	3.40 ± 0.10	$3600 \pm 8\%$	$129 \pm 10\%$	$3.35 \pm 10\%$	0.74 ± 0.10
α Sco	$180 \pm 15\%$	4.76 ± 0.12	$3400 \pm 6\%$	$703 \pm 15\%$	$12 \pm 20\%$	-0.18 ± 0.11
α^1 Her	$120 \pm 15\%$	3.92 ± 0.15	$2800 \pm 10\%$	$387 \pm 20\%$	$2.15 \pm 10\%$	-0.41 ± 0.19
α Ori [A]	$131 \pm 20\%$	4.73 ± 0.15	$3340 \pm 6\%$	$695 \pm 20\%$	$10 \pm 20\%$	-0.25 ± 0.23
α Ori [B]	$131 \pm 20\%$	4.81 ± 0.15	$3650 \pm 10\%$	$637 \pm 20\%$	$10 \pm 20\%$	-0.17 ± 0.14

Notes: The estimated relative uncertainties are given in % or dex. Relationships between the uncertainties are considered, if applicable. For instance, if the distance d is uncertain, the radius R_* scales as $\propto d$ and the luminosity L_* as $\propto d^2$.

$BC = 0.1$. Furthermore, these properties compare well with an evolution model for a $2.1M_\odot$ mass star at an advanced age of about $9 \cdot 10^8$ yr. These values for the age and distance of the system are well consistent with the evolution model for α^2 Her A, a G9 III giant of $2.40M_\odot$ with $T_{\text{eff}} = 4900$ K (Thiering & Reimers 1993) and $\log L_*/L_\odot = 2.03$ (for $V = 5.6$ and $BC = 0.46$). These good matches (see Fig. 4) therefore confirm the Hipparcos distance of 120 pc and, consequently, we adopt a reduced uncertainty, i.e., about 15%.

Recently, Levesque et al. (2005) [LMO05] derived $T_{\text{eff}} = 3450$ K, $BC = 2.49$ and $A_v = 1.40$ for the M-type giant primary α^1 Her by detailed atmospheric modelling using the strengths of the TiO bands. The resulting physical properties are given in Table 5, assuming a distance of 120 pc and $V = 3.2$ for the M supergiant alone (with $V = 3.06$ for the system of α Her, according to SIMBAD). In general, the M-type T_{eff} -scale by Levesque et al. (2005) is less cool, and BC values are less large (but accompanied by unusually large A_v values), as those of many other authors. In the case of α^1 Her, this does not result in a smaller radius, however. It would be $R \approx 410R_\odot$, considering the unusually large absorption of $A_v = 1.4$ required by Levesque et

al. (2005) to attain a consistent atmospheric model. This implies, at the same time, a much larger luminosity.

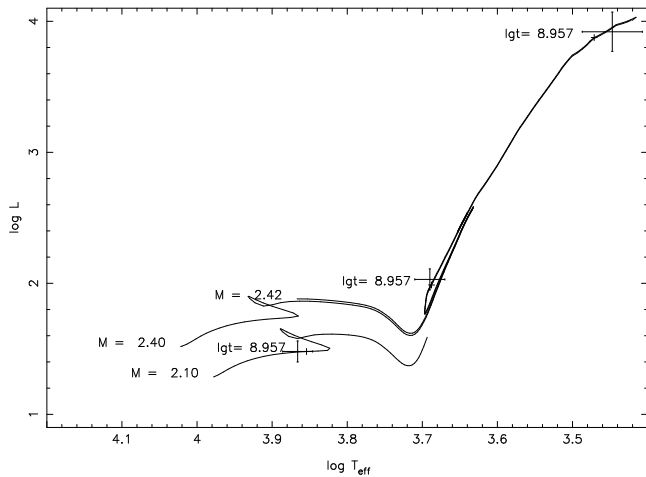
The LBI-measured angular diameter in the V band (UDD; see Richichi & Percheron 2002) of 30 mas yields a radius of $387 R_\odot$ (for $d = 120$ pc). Hence, based on this empirical angular diameter, we adopt the following parameters for α^1 Her (Table 5): With $V = 3.2$ for the M-giant alone and a combined BC and A_v of 2.9, we find $\log L_*/L_\odot = 3.92$. With a radius of $387 R_\odot$, we then derive $T_{\text{eff}} = 2800$ K, which is in reasonable agreement with near tip-AGB evolution models. The M supergiant's mass can also be well constrained (within about 10%), since α^1 Her must have evolved from a star of slightly larger initial mass than the G9 giant, i.e., about $2.4 M_\odot$. Therefore, we obtain a present mass of $2.15 M_\odot$, considering the mass loss given by our evolution model (see Fig. 4). Based on these values, we find a surface gravity of $\log g = -0.41 \pm 0.19$ (cgs).

The aforementioned mass-loss rates derived from the line-of-sight absorption of wind-lines scale linearly with the system dimensions, which in this case are proportional to the adopted values of d . Hence, a distance of $d = 120$ pc yields observed mass-loss rates of $2.2 \cdot 10^{-7}$ and $2.6 \cdot 10^{-7} M_\odot \text{ yr}^{-1}$ for the studies of Reimers (1977) and Thiering &

Table 8. Observed versus predicted mass-loss rates in $\log(M_{\odot} \text{ yr}^{-1})$.

Reference	α Boo	32 Cyg	δ Sge	α Sco	α^1 Her	α Ori [A]	α Ori [B]
R75	-9.14 ± 0.03	-7.49 ± 0.07	-7.71 ± 0.14	-6.18 ± 0.13	-6.52 ± 0.14	-6.13 ± 0.14	-6.09 ± 0.17
L81	-8.83 ± 0.03	-6.85 ± 0.10	-7.19 ± 0.20	-5.37 ± 0.16	-5.97 ± 0.20	-5.33 ± 0.19	-5.24 ± 0.21
dJNH88	...	-7.15 ± 0.11	-7.53 ± 0.33	-6.05 ± 0.11	-6.27 ± 0.36	-6.09 ± 0.19	-5.95 ± 0.17
NdJ90	-9.73 ± 0.03	-6.62 ± 0.10	-7.40 ± 0.20	-4.78 ± 0.18	-6.30 ± 0.21	-4.84 ± 0.21	-4.76 ± 0.23
SC05	-9.38 ± 0.03	-7.63 ± 0.10	-7.94 ± 0.20	-5.81 ± 0.25	-6.23 ± 0.29	-5.71 ± 0.29	-5.60 ± 0.34
Observed	-9.60 ± 0.3	-7.82 ± 0.2	-7.85 ± 0.3	-5.82 ± 0.3	-6.50 ± 0.3	-5.51 ± 0.2	-5.51 ± 0.2

Notes: The estimated uncertainties of the observed and predicted values are given in dex. For R75, $\eta_{\text{R}} = 2 \cdot 10^{-13}$ is used (see Schröder & Cuntz 2005).

**Fig. 4.** Observed HRD positions of the three components of α Her and evolution tracks of 2.10, 2.40 and 2.42 M_{\odot} (initial) mass, using a metallicity of $Z = 0.02$.

Reimers (1993), respectively. The rate derived by Maun & Caux (1992), however, scales with the distance squared, since it is based on emission measure, and thus translates into $4.0 \cdot 10^{-7} M_{\odot} \text{ yr}^{-1}$. Consequently, we adopt $3.0 \cdot 10^{-7} M_{\odot} \text{ yr}^{-1}$, which is considered uncertain by a factor of 2.

With the adopted physical parameters for α^1 Her, our new mass-loss relation (Schröder & Cuntz 2005) results in a mass-loss rate of $5.9 \cdot 10^{-7} M_{\odot} \text{ yr}^{-1}$, while the old “Reimers law” (with $\eta_{\text{R}} = 2 \cdot 10^{-13}$) yields $3.0 \cdot 10^{-7} M_{\odot} \text{ yr}^{-1}$ — see Table 8, also for other mass-loss predictions. In this particular case, it seems that the old “Reimers law” is more accurate than our new relation. Nonetheless, both mass-loss predictions are consistent with the observed value within the uncertainty bars. Furthermore, if in fact T_{eff} were larger by 10%, which is principally possible, and hence the radius were smaller by 20%, our new relation would result in the closer match.

2.6. α Ori (*M2 lab*)

A good test candidate for the various empirical mass-loss formulas is the well-studied massive cool supergiant α Ori (Betelgeuse). Betelgeuse has some circumstellar dust, but it is considered to be not dynamically important, owing to the

fact that Betelgeuse’s luminosity is just below its critical luminosity value to initiate a truly dust-driven wind.

Mass-loss rates derived from observation have improved a lot since, e.g., Judge & Stencel (1991) [JS91], when models based on the total line flux were used. A mass-loss rate of $3.1(\pm 1.3) \cdot 10^{-6} M_{\odot} \text{ yr}^{-1}$ has been derived by Harper et al. (2001) [HBL01], using spatially resolved radio flux data and assuming a distance of $d = 131 \text{ pc}$ ($\pm 20\%$), based on the Hipparcos parallax. From spectrophotometry, they also derive a corresponding luminosity of $L_* = 5.35 \cdot 10^4 L_{\odot}$, or $M_{\text{bol}} = -7.10$, implying a combined BC and A_v of 2.1 ($V = 0.6$). With an angular diameter (based on the purely empirical UDD) of $56 (\pm 1) \text{ mas}$, they find $R_* = 789 R_{\odot}$ and $T_{\text{eff}} = 3140 \text{ K}$. By contrast, Levesque et al. (2005) [LMO05] find $T_{\text{eff}} = 3650 \text{ K}$ and suggest $A_v = 0.62$. On their BC -scale α Ori would require about 1.60. In Table 6, we list all relevant physical properties, following Levesque et al. and based on a distance of 131 pc, hereafter referred to as α Ori Model B.

However, the resulting radius of the spectroscopy-based Model B, $637 R_{\odot}$, is too small to be consistent with the most accurate and purely empirical UDD (LBI, 800 nm): Richichi & Percheron (2002) list α Ori’s angular diameter as $49.4 \pm 0.24 \text{ mas}$, suggesting a radius of $695 R_{\odot}$ at the same 131 pc distance. This purely empirical radius implies $T_{\text{eff}} = 3340 \text{ K}$, as listed in Table 6 as α Ori Model A, based on the above LBI measurement. Since our best-matching evolution track suggests a mass of $M_* \simeq 10 M_{\odot}$ ($\pm 20\%$) for α Ori, the corresponding values for the surface gravity are $\log g = -0.25 \pm 0.23$ (cgs) (Model A) and -0.17 ± 0.14 (cgs) (Model B).

For testing the mass-loss relations, we here proceed with both models, A and B, in order to properly reflect the whole range of parameters produced by the wealth of observations on this particular star. For Model A, the new mass-loss relation by Schröder & Cuntz (1995) yields $2.0 \cdot 10^{-6} M_{\odot} \text{ yr}^{-1}$, which is consistent with the observed value of $3.1 \cdot 10^{-6}$ within the uncertainty bars, while the “Reimers law” (with $\eta_{\text{R}} = 2 \cdot 10^{-13}$) gives $7.4 \cdot 10^{-7} M_{\odot} \text{ yr}^{-1}$. If Model B is adopted, the mass-loss relation by Schröder & Cuntz yields $2.5 \cdot 10^{-6} M_{\odot} \text{ yr}^{-1}$, while the original “Reimers law” yields $8.1 \cdot 10^{-7} M_{\odot} \text{ yr}^{-1}$. In both cases, the new relation by Schröder & Cuntz (2005) matches the observations very well, while the old “Reimers law” suggests rates significantly too low. In fact, the new relation by Schröder & Cuntz is best among all tested relations, regardless whether Model A or Model B is selected (see Table 8). The predictions by the other mass-loss relations are consistently too

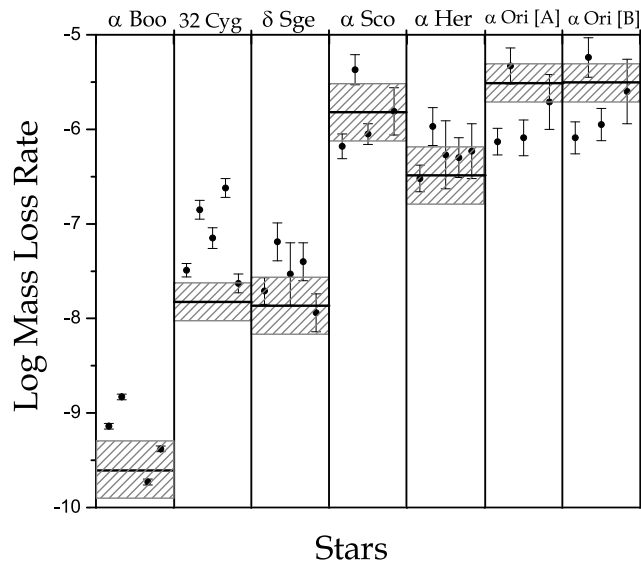


Fig. 5. Comparison of observed (thick horizontal lines, uncertainties indicated by dashed areas) and predicted mass-loss rates (with error bars) for our target stars, as given in Table 8. The different predicted mass-loss rates follow, for each star, the sequence R75, L81, dJNH88, NdJ90, and SC05, from l.t.r. Note that only the values given by SC05 agree with the observations in *all* cases.

low or too high, and are mostly well outside the combined observational and theoretical uncertainties.

3. Conclusions

It has been the aim of this paper to check the quality of our new, improved Reimers-type mass-loss law given by Schröder & Cuntz (2005). For this purpose, we considered a set of well-studied giant and supergiant stars, which are: α Boo (K1.5 III), 32 Cyg (K5 Ib), δ Sge (M2 II), α Sco (M1.5 Iab), α^1 Her (M5 Ib), and α Ori (M2 Iab). These stars, except α Boo, have spatially resolved circumstellar shells and winds — obtained directly or by means of a companion acting as a probing light source — resulting in relatively accurate, empirically determined mass-loss rates. In addition, they encompass a significant range in luminosity (factor of 400), stellar radius (factor of 30), and stellar mass (factor of 10). As comparison, we used the empirical mass-loss relations given by Reimers (1975), Lamers (1981), de Jager et al. (1988) and Nieuwenhuijzen & de Jager (1990).

As part of the comparison, we considered updated stellar parameters, including stellar masses, which have been constrained using detailed stellar evolution computations. Further updates include recent angular diameter measurements and stellar spectral analyses. In addition, we considered parallax determinations by Hipparcos resulting in improved values for the stellar luminosities. For all of our target stars, we find that the mass-loss rates suggested by the relation by Schröder & Cuntz (2005) comfortably agree with the observed values within the uncertainty bars. This is often not the case for the other mass-loss relationships considered here (see Fig. 5). In many cases, those predictions are much too high or much too low, without any sys-

tematic trend in regard to the relationship or the target star. The uncertainty bars of the empirical predictions were obtained based on a detailed error propagation analysis also considering any mutual dependencies of variable such as L_* , R_* , and T_{eff} .

Hence, we presented detailed empirical evidence in support of the new Reimers-type mass-loss relation by Schröder & Cuntz (2005), which we now feel safe to recommend for application to moderate, cool (i.e., not dust-driven) stellar winds. However, we like to caution that this new relation shall not be applied to predict the rates of stellar mass-loss physically very different from moderate, cool winds — especially not to hot radiation-driven winds, coronal mass-loss, pulsation-driven winds, and massive dust-driven winds.

Our future efforts will also include to investigate whether an underlying Reimers-type mass-loss mechanism could provide vital *initial* energy input for the non-pulsating dust-driven winds of the coolest AGB giants. After all, any efficient dust-formation relies on a supplementary mechanism needed to carry sufficient matter from the stellar photosphere to the dust formation radius. Such a mechanism is needed to ensure a sufficiently high optical depth at the inner boundary of the mass-loss region, initiating massive mass loss by radiative pressure on the dust.

Acknowledgements. This work has partially been supported by NSF grant ATM-0538278 (M. C.). We also acknowledge support by L. Gurdemir for his assistance with computer graphics, and we wish to thank the anonymous referee for his helpful comments.

References

- Airapetian, V. S., Ofman, L., Robinson, R. D., Carpenter, K., & Davila, J. 2000, *ApJ*, 528, 965
 Ayres, T. R., & Linsky, J. L. 1975, *ApJ*, 200, 660
 Ayres, T. R., Brown, A., & Harper, G. M. 2003, *ApJ*, 598, 610
 Baade, R. 1990a, *A&A*, 233, 486
 Baade, R. 1990b, in *Evolution in Astrophysics*, ESA SP-310, 65 (B90)
 Baade, R. 1998, in *Ultraviolet Astrophysics: Beyond the IUE Final Archive*, ESA SP-413, 325
 Baade, R., Kirsch, T., Reimers, D., Brown, A., Bennett, P., & Harper, G. 2001, in *Cool Stars, Stellar Systems and the Sun XI*, ed. R. J. García López, R. Rebolo, & M. R. Zapatero Osorio (San Francisco: ASP), vol. 223, 1585 (B01)
 Charbonnel, C., Brown, J. A., & Wallerstein, G. 1998, *A&A*, 332, 204
 Che, A., Hempe, K., & Reimers, D. 1983, *A&A*, 126, 225 (CHR83)
 Cuntz, M. 1990, *ApJ*, 349, 141
 Decin, L., Vandenbussche, B., Waelkens, C., Decin, G., Eriksson, K., Gustafsson, B., Plez, B., & Sauval, A. J. 2003, *A&A*, 400, 709 (DVW03)
 de Jager, C., Nieuwenhuijzen, H., & van der Hucht, K. A. 1988, *A&AS*, 72, 259 (dJNH88)
 Drake, S. A. 1985, in *Progress in Stellar Spectral Line Formation Theory*, ed. J. E. Beckman & L. Crivellari (Dordrecht: Reidel), 351
 Drake, S. A., & Linsky, J. L. 1983, *ApJ*, 274, L77
 Drake, S. A., & Linsky, J. L. 1986, *AJ*, 91, 602
 Eggleton, P. P. 1971, *MNRAS*, 151, 351
 Erhorn, G. 1990, Ph.D. thesis, University of Hamburg
 Griffin, R. E. M., & Lynas-Gray, A. E. 1999, *AJ*, 117, 2998 (GLG99)
 Judge, P. G., & Stencel, R. E. 1991, *ApJ*, 371, 357 (JS91)
 Hagen, H.-J., Hempe, K., & Reimers, D. 1987, *A&A*, 184, 256 (HHR87)
 Harper, G. M., Brown, A., & Lim, J. 2001, *ApJ*, 551, 1073 (HBL01)
 Hartmann, L., & Avrett, E. H. 1984, *ApJ*, 284, 238
 Hjellming, R. M., & Newell, R. T. 1983, *ApJ*, 275, 704 (HN83)
 Kudritzki, R. P., & Reimers, D. 1978, *A&A*, 70, 227 (KR78)
 Lamers, H. J. G. L. M. 1981, *ApJ*, 245, 593 (L81)
 Levesque, E. M., Massey, P., Olsen, K. A. G., Plez, B., Josselin, E., Maeder, A., & Meynet, G. 2005, *ApJ*, 628, 973 (LMO05)
 Malmquist, K. G. 1936, *Stockholm Obs. Medd. No. 26*
 Maun, N., & Caux, E. 1992, *A&A*, 265, 711

- Musielak, Z. E. 2004, in Stars as Suns: Activity, Evolution and Planets, IAU Symp. 219, ed. A. K. Dupree & A. O. Benz (San Francisco: ASP), 437
- Nieuwenhuijzen, H., & de Jager, C. 1990, A&A, 231, 134 (NdJ90)
- Pols, O. R., Tout, C. A., Schröder, K.-P., Eggleton, P. P., & Manners, J. 1997, MNRAS, 289, 869
- Press, W. H., Flannery, B. P., Teukolsky, S. A., & Vetterling, W. T. 1986, Numerical Recipes (Cambridge: Cambridge Univ. Press)
- Reimers, D. 1975, Mem. Roy. Soc. Liège 6. Ser. 8, 369 (R75)
- Reimers, D. 1977, A&A, 61, 217 [Erratum: 67, 161] (R77)
- Reimers, D., & Schröder, K.-P. 1983, A&A, 124, 241 (RS83)
- Richichi, A., & Percheron, I. 2002, A&A, 386, 492
- Schröder, K.-P. 1983, A&A, 124, L16
- Schröder, K.-P., Pols, O. R., & Eggleton, P. P. 1997, MNRAS, 285, 696 (SPE97)
- Schröder, K.-P., Winters, J. M., & Sedlmayr, E. 1999, A&A, 349, 898
- Schröder, K.-P., & Sedlmayr, E. 2001, A&A, 366, 913
- Schröder, K.-P., Wachter, A., & Winters, J. M. 2003, A&A, 398, 229
- Schröder, K.-P., & Pagel, B. E. J. 2003, MNRAS, 343, 1231
- Schröder, K.-P., Pauli, E.-M., & Napiwotzki, R. 2004, MNRAS, 354, 727
- Schröder, K.-P., & Cuntz, M. 2005, ApJ, 630, L73 (SC05) (Paper I)
- Taylor, B. J. 1999, A&AS, 134, 523
- Thiering, I., & Reimers, D. 1993, A&A, 274, 838 (TR93)
- van der Hucht, K. A., Bernat A. P., & Kondo Y. 1980, A&A, 82, 14
- Wright, K. O. 1970, Vistas in Astronomy, 12, 147